Journal of Southeast University (English Edition) Vol. 32, No. 1, pp. 73 - 77 Mar. 2016 ISSN 1003—7985

Dynamic caustics experimental study on interaction between propagating crack and deformity inclusions in primary structure

Yue Zhongwen[1] Han Ruijie[1] Zhang Wang[1] Liu Wei[2]

([1]School of Mechanics and Civil Engineering, China University of Mining and Technology, Beijing 100083, China)
([2]Department of Engineering Mechanics, Tsinghua University, Beijing 100084, China)

Abstract: The approach combining the dynamic caustics method with high-speed photography technology is used to study the interaction between propagating cracks and three kinds of deformity inclusions (cylinder inclusion, quadruple inclusion and triangular inclusion) under low velocity impact loading. By recording the caustic spots of crack tips at different moments during the crack propagation, the variation regulations of dynamic stress intensity factors (DSIF) and crack growth velocity with respect to time are obtained. The experimental results show that the resistance effects to crack growth are varied with different shapes of inclusions in specimens, and the quadruple inclusion's effect is more apparent. The distortion degree of caustic spots is affected by the shapes of inclusions as well, and the situation is more serious for cylinder and quadruple inclusions. The overall values of DSIFs of triangular inclusion specimen are greater than the others, and the crack growth velocities, characteristic sizes and DSIFs show processes of fluctuations because of the disturbance of reflection waves in specimens. The results provide an experimental basis for the analysis of strength and impact-resistance ability in structures with deformity inclusions.

Key words: dynamic caustics; deformity inclusion; dynamic stress intensity factor (DSIF); crack propagation velocity
DOI: 10.3969/j.issn.1003 - 7985.2016.01.013

It is well known that various inclusions are inevitable in many engineering structures. Under impact loading, these inclusions will directly influence the crack path, the crack velocity and the stress intensity factors at the crack tip[1-2]. How to evaluate the dynamic interaction between the inclusions and the propagating cracks is still a difficult academic problem, which is important for characterizing the strength and predicting the lifetime of the engineering components with inclusions.

Optical caustics technology in combination with high-speed photography has been widely applied for investigating the dynamic fracture behaviors of engineering materials and structures[3-7]. Theocaris et al.[8-9] studied the crack propagation behavior of the quasi-static crack tip field using the caustics method. Beinert et al.[10] applied the caustics method to the experimental study of dynamic fracture mechanics by introducing a correction factor and determined the stress intensity factor at the crack tip successfully. Jajam et al.[11] simulated the dynamic crack propagation of specimens with flexible and rigid inclusions. Yao et al.[12-13] studied the multiple cracks interaction in polymer materials and the crack tip stress singularity in composite by the caustics experimental method. Li et al.[14-15] applied the caustics method in the fracture mechanics analysis of orthotropic composites and viscoelastic materials.

However, there is still very little research regarding the influences of inclusions in various shapes on a crack's development and propagation, which will probably cause the unstability of engineer components and then pose a hidden danger for the whole project. Therefore, in this paper, the interactions between the propagating cracks and deformity inclusions are studied by means of the dynamic caustics method for the purpose of providing a theoretical basis for the actual projects. Dynamic caustic patterns surrounding the propagating crack tip of the specimen with the inclusion such as cylinder, quadruple prisms and triple prisms are recorded by a high-speed camera. Some dynamic fracture parameters such as the dynamic stress intensity factor and the crack velocity are obtained, and the influence mechanism of deformity inclusions on the fracture parameters is also stated.

1 Experimental Details

1.1 Specimen with inclusion

The epoxy resin specimen with 150 mm × 40 mm × 5 mm in length × width × thickness is prepared. Three kinds of inclusions (they are actually holes in different shapes) are cured inside the epoxy resin specimen, such as cylinder with 5 mm × 10 mm in thickness × diameter, quadruple prisms with 5 mm × 10 mm in thickness × length of a side and triple prisms with 5 mm × 10 mm in thickness × length of a side. The geometrical configuration of the final specimen is shown in Fig. 1. The initial

Received 2015-08-30.
Biography: Yue Zhongwen (1975—), male, doctor, associate professor, zwyue75@163.com.
Foundation items: The National Natural Science Foundation of China (No. 51374210, 51134025), the 111 Project (No. B14006).
Citation: Yue Zhongwen, Han Ruijie, Zhang Wang, et al. Dynamic caustics experimental study on interaction between propagating crack and deformity inclusions in primary structure[J]. Journal of Southeast University (English Edition), 2016, 32(1): 73 - 77. DOI: 10.3969/j.issn.1003 - 7985.2016.01.013.

crack is 5 mm × 0.8 mm in length × width, and the distance between the initial crack tip position and the bottom of the inclusion is 10 mm. The impact system is shown in Fig. 2.

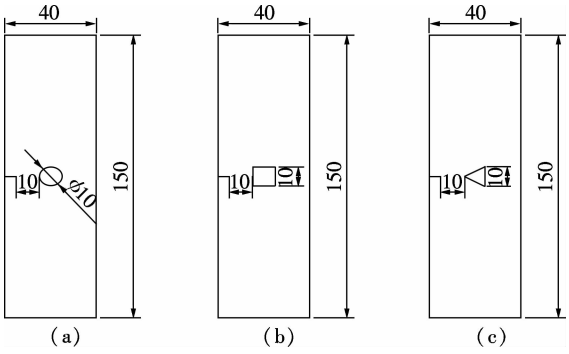

Fig. 1 Three kinds of specimens containing different inclusions (unit: mm). (a) Cylinder; (b) Quadruple prisms; (c) Triple prisms

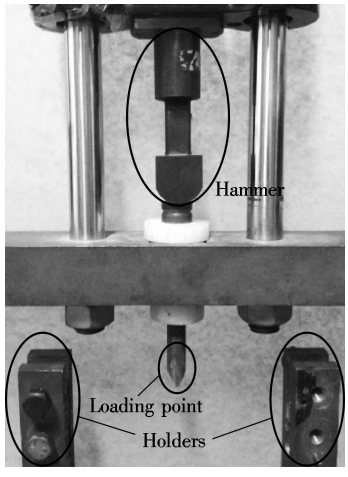

Fig. 2 Impact system

1.2 Digital laser dynamic caustics experimental system

A digital laser dynamic caustics experimental system is shown in Fig. 3, including the laser, optical lens, low velocity impact system and high speed camera (Fastcam-SA5-16G, Photron Company, Japan). In this study, the photograph resolution is 128 × 64 pixels; the pixel-to-length ratio of the images is 1.8 and the pump laser power is 50 mW. The high-speed camera is used to record different transient moment caustic spots around the propagating crack tip under low velocity impact loading. A green laser light source is used as an illumination for dynamic optical recording.

First, the specimen was placed onto the holders to have them fixed, and the hammer of 1 kg was raised to 500 mm (the final velocity was nearly 3.13 m/s) above the upper surface of the specimen. Secondly, the laser was initiated and the optical path was calibrated to make sure that the image shown in the high speed camera was clear and complete; the interval of the high speed camera was set to be 3 μs. Finally, the crack tip of the initial crack began to accumulate energy when the hammer impacted on the

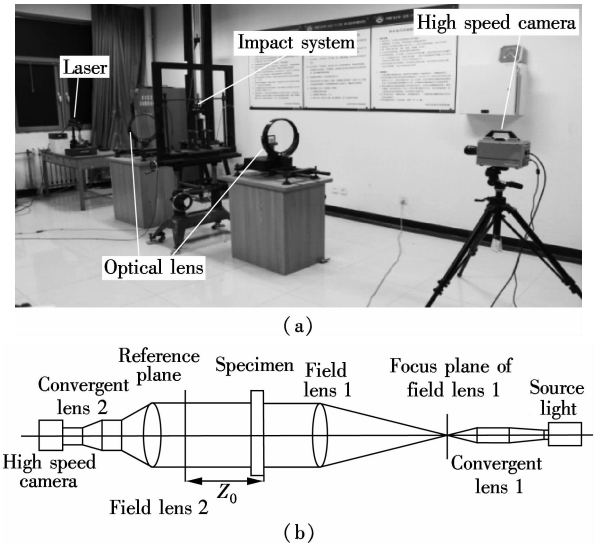

Fig. 3 Digital laser dynamic caustics experimental system. (a) Experimental setup; (b) Optical arrangement

specimen. Once the energy reached the required value for crack development, the initial crack was initiated and propagated under impact loading. By using the high speed camera, the caustic spots of the crack tip during the process of propagating were recorded, which were the basis for calculating the characteristic sizes, crack velocities and dynamic stress intensity factors.

1.3 Dynamic stress intensity factor

Based on the dynamic caustics experiments of mode Ⅰ crack, the dynamic stress intensity factor K_{I}^{d} at the propagating crack tip can be expressed as[10]

$$K_{\mathrm{I}}^{d}=\frac{2\sqrt{2\pi}F(v)}{3(3.17)^{5/2}Z_0 c d_{\mathrm{eff}}}d^{5/2} \tag{1}$$

where d is the maximum transverse diameter of the caustic at the crack tip; Z_0 is the distance between the reference plane and the specimen plane; c is the dynamic stress optical constant of materials; d_{eff} is the effective thickness of the specimen; $F(v)$ is a velocity correction factor in dynamic caustics experiments, which can be expressed as

$$F(v)=\frac{4\beta_{\mathrm{d}}\beta_{\mathrm{s}}-(1+\beta_{\mathrm{s}}^{2})}{(1+\beta_{\mathrm{s}}^{2})(\beta_{\mathrm{d}}^{2}-\beta_{\mathrm{s}}^{2})} \tag{2}$$

where $\beta_i^2=1-(v/c_i)^2$, $i=\mathrm{d},\ \mathrm{s}$; c_{d} and c_{s} represent the expansion wave and shear wave velocity of epoxy resin, respectively; v is the crack instantaneous growth velocity. When the crack is not initiated, $v=0$, $F(v)=1$.

In this experiment, $Z_0=500$ mm, $c=0.77\times10^{-10}$ m^2/N, and $d_{\mathrm{eff}}=5$ mm. Once the maximum transverse diameter at the crack tip is measured, the dynamic stress intensity factor of the model Ⅰ crack tip can be calculated according to Eqs. (1) and (2). The mechanical properties of epoxy resin are shown in Tab. 1.

Tab. 1 Dynamic mechanical parameters of epoxy resin specimens

Parameter	C_d/(m · s^{-1})	C_s/(m · s^{-1})	E_d/GPa	v	c/(m^2 · N^{-1})
Value	2 320	1 260	3.7	0.36	0.77×10^{-10}

2 Experimental Results and Analysis

2.1 Dynamic fracture patterns on specimens with deformity inclusions

Dynamic caustic patterns at the crack tip for the specimen with the inclusion like triple prisms, cylinder and quadruple prisms under low velocity impact loading are shown in Fig. 4, Fig. 5 and Fig. 6, respectively.

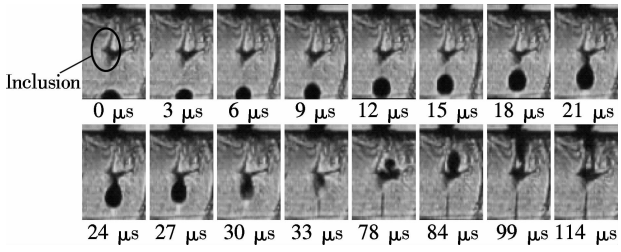

Fig. 4 Dynamic caustic patterns on specimen with triple prisms inclusion

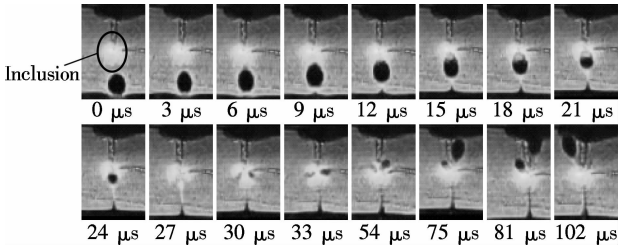

Fig. 5 Dynamic caustic patterns on specimen with cylinder inclusion

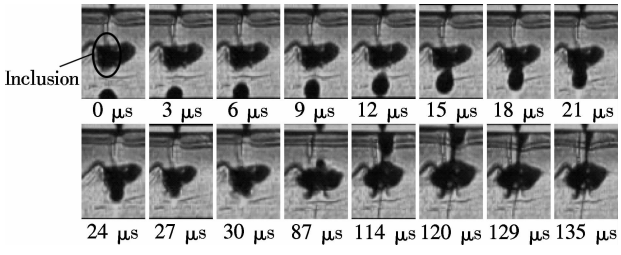

Fig. 6 Dynamic caustic patterns on specimen with quadruple prisms inclusion

As shown in Fig. 4, when $t = 0$ to 12 μs, the evolution of the caustic spot at the crack tip is almost the same as that in the homogenous material. While the crack tip gradually closes to the triple prisms inclusion from $t = 15$ μs to $t = 33$ μs, the influences of the triple prisms inclusion on the crack tip caustic spot are obvious. Then, the crack tip makes contact with the triple prisms inclusion and expands along the interface of it and the epoxy resin material, and the caustic spot arises irregularly at this time. This is because the crack is not under mode Ⅰ loading and the stress state around the crack tip is more complex. When $t > 78$ μs, the crack tip crosses through the triple prisms inclusion completely until it extends through the whole specimen.

For the dynamic fracture on the specimen with cylinder inclusion as shown in Fig. 5, the influences of cylinder inclusion on the crack tip caustic spot become significant when $t = 3$ μs, and then the shape of the crack tip caustic spot continues to distort under the influence of the cylinder inclusion. What needs to be noticed is that the cylinder inclusion shows a significant crack-arrest influence on the growing crack before 30 μs. The caustic spot becomes smaller as the crack reaches the lower edge of the cylinder inclusion. When $t = 27$ μs, the caustic spot vanishes because of the strong fracture resistance. When $t > 30$ μs, the crack restarts to accumulate the energy, then it develops surrounding the cylinder inclusion and the crack extends along both sides of the inclusion interface. The right crack expands faster and continues to propagate after reaching the inclusion's upper boundary. Subsequently, the left crack passes through the inclusion and expands upwards at a certain angle long with the loading direction. As the right crack crosses through the specimen, the left caustic spot of the crack tip decreases. Ultimately, the left crack fails to cross through the specimen.

As shown in Fig. 6, in the early stage of crack expansion, the quadruple prism inclusion has smaller effect on the crack tip caustic spot. With the crack expanding, the influence of the quadruple prism inclusion tends to be obvious, and the shape of the crack tip caustic spot is significantly stretched along the direction of crack expansion. After passing through the quadruple prisms inclusion, the crack expands to the top of the specimen.

On the whole, the crack tip caustic spots of the specimens with deformity inclusions undergo a distortion process before the crack meets the inclusions under impact loading. Cylinder inclusion and quadruple prisms inclusion pose greater influences on the crack caustic spots than triple prism inclusion. The reason for this phenomenon is that the stress wave at the crack tip is released after the crack initiation, and the crack tip caustic spot is influenced by the wave reflection of the specimen boundary and mixed interface. The final fracture patterns of three kinds of specimens are shown Fig. 7.

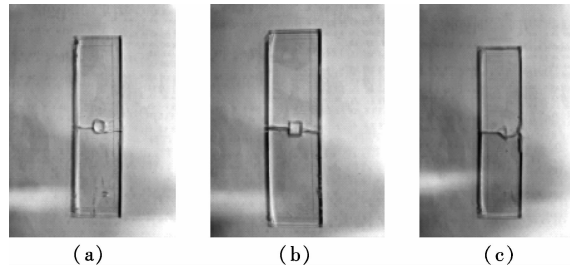

Fig. 7 Fracture patterns of three kinds of specimens containing deformity inclusions. (a) Cylinder; (b) Quadruple prisms; (c) Triple prisms

2.2 Crack growth velocity

Before the crack tip expands to the inclusion, the crack growth velocity v varies with time t as shown in Fig. 8. It can be seen that, with the crack initiation of specimens with deformity inclusions, the crack growth velocities of three kinds of specimens all rise in an obvious trend, which runs up to the first peaks at 9 to 12 μs, respectively, then the crack growth velocities fluctuate up and down. For deformity inclusions, the frequencies and angles of reflection stress waves are different; therefore, the crack growth velocities of these specimens with deformity inclusions are different.

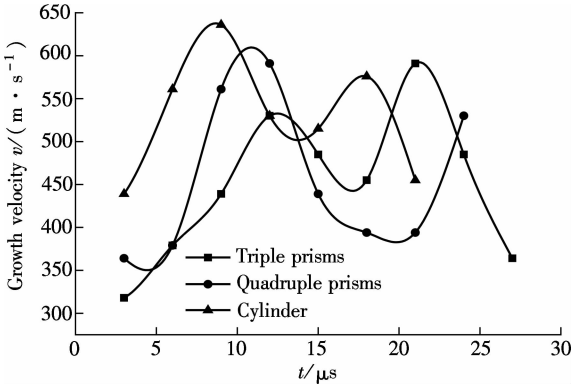

Fig. 8 The growth velocity v of cracks

2.3 Dynamic stress intensity factor

Before the crack meets inclusion, both the characteristic size d of caustic spots and the dynamic stress intensity factor K_I^d of specimens with deformity inclusions are shown in Fig. 9 and Fig. 10, respectively.

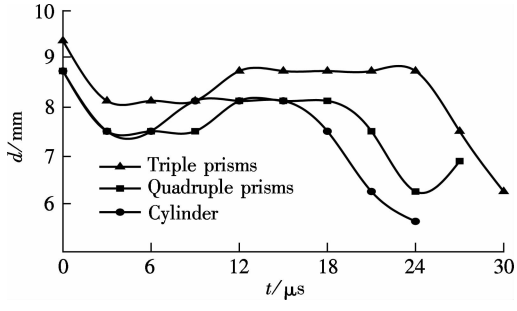

Fig. 9 Characteristic size d of caustic spots

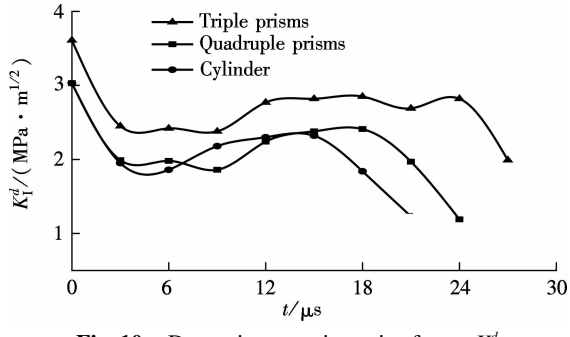

Fig. 10 Dynamic stress intensity factor K_I^d

From Fig. 9 and Fig. 10, when the crack initiates, the characteristic size d of caustic spots and the dynamic stress intensity factor K_I^d of specimens with deformity inclusions are all decreased, and the decreasing extents are basically the same. With the propagation of the crack, the dynamic stress intensity factor begins to fluctuate. The reason is that the stress wave that the crack tip releases along the expansion of crack experiences multiple reflections by the specimen as well as a mixed boundary, and subsequently acts on the crack tip and superimposes on the releasing stress wave of the crack tip. Eventually, the stress intensity factors happen to fluctuate due to the complex interactions between stress waves. Simultaneously, the dynamic stress intensity factor of the specimen with the triple prism inclusion is greater than those of specimens with quadruple prism inclusion and cylinder inclusion, and the dynamic stress intensity factor of the specimens with quadruple prism inclusion and cylinder inclusion are almost similar. In other words, the influence of the reflecting stress wave on the crack tip stress field is the most remarkable in the specimen with triple prism inclusion.

3 Conclusion

1) Inclusions in different shapes have different effects on the fracture resistance of the crack's development and propagation. The quadruple prism and cylinder inclusions pose greater influence on the propagating crack than triple prism inclusion does.

2) The reflection effect of deformity inclusions on the stress wave is different, and thus the distortion degree of caustic spot varies with the shapes of the inclusions. Specimens containing cylinder inclusion and quadruple prism inclusion distort the caustic spots of the crack tips more seriously than those with triple prisms do.

3) The dynamic stress intensity factors show fluctuation because of the disturbance of the reflecting stress wave to the crack tip. The overall dynamic stress intensity factors of the specimen containing triple prism are higher than those with cylinder inclusion and quadruple prism inclusion at the same moment. In other words, the reflecting stress wave in the specimens of triple prism inclusion has a greater influence on the stress field.

References

[1] Yao X F, Xu W. Recent application of caustics on experimental dynamic fracture studies[J]. *Fatigue & Fracture of Engineering Materials & Structures*, 2011, **34**(6): 448 - 459.

[2] Rosakis A J. Analysis of the optical method of caustics for dynamic crack propagation[J]. *Engineering Fracture Mechanics*, 1980, **13**(2): 331 - 347. DOI: 10.1016/0013-7944(80)90063-6.

[3] Yang R S, Yue Z W, Sun Z H, et al. Dynamic fracture behavior of rock under impact load using the caustics

method[J]. *Mining Science and Technology*, 2009, **19**(1): 79-83. DOI: 10.1016/S1674-5264(09)60015-6.
[4] Yao X F, Xu W, Xu M Q, et al. Experimental study of dynamic fracture behavior of PMMA with overlapping offset-parallel cracks[J]. *Polymer Testing*, 2003, **22**(6): 663-670.
[5] Yao X, Chen J, Jin G, et al. Caustic analysis of stress singularities in orthotropic composite materials with mode-Ⅰ crack[J]. *Composites Science & Technology*, 2004, **64**(7/8): 917-924.
[6] Yue Z W, Yang R S, Sun Z H, et al. Impact fracture experiment of crack rock with inclined edge[J]. *Journal of Coal Science & Engineering (China)*, 2010, **35**(9): 1456-1460. (in Chinese)
[7] Papadopoulos G A, Papanicolaou G C. Dynamic crack propagation in rubber-modified composite models[J]. *Journal of Materials Science*, 1988, **23**(10): 3421-3434. DOI: 10.1007/BF00540474.
[8] Theocaris P S, Katsamanis P. Response of cracks to impact by caustics[J]. *Engineering Fracture Mechanics*, 1978, **10**(2):197-210.
[9] Katsamanis F, Raftopoulos D, Theocaris P S. Static and dynamic stress intensity factors by the method of transmitted caustics[J]. *Journal of Engineering Materials and Technology*, 1977, **99**(2): 105-109. DOI:10.1115/1.3443417.
[10] Beinert J, Kalthoff J F. Experimental determination of dynamic stress intensity factors by shadow patterns[M]//*Experimental Evaluation of Stress Concentration and Intensity Factors*. Berlin: Springer, 1981: 281-330.
[11] Jajam K C, Tippur H V. Role of inclusion stiffness and interfacial strength on dynamic matrix crack growth: An experimental study[J]. *International Journal of Solids and Structures*, 2012, **49**(9): 1127-1146. DOI: 10.1016/j.ijsolstr.2012.01.009.
[12] Yao X F, Jin G C, Arakawa K, et al. Experimental studies on dynamic fracture behavior of thin plates with parallel single edge cracks[J]. *Polymer Testing*, 2002, **21**(8): 933-940.
[13] Yao X F, Xu W, Jin G C, et al. Low velocity impact study of laminate composites with mode Ⅰ crack using dynamic optical caustics[J]. *Journal of Reinforced Plastics & Composites*, 2004, **23**(17): 1833-1844.
[14] Gong K Z, Li Z. Caustics method in dynamic fracture problem of orthotropic materials[J]. *Optics and Lasers in Engineering*, 2008, **46**(8): 614-619. DOI: 10.1016/j.optlaseng.2008.03.019.
[15] Gao G Y, Li Z, Xu J. Optical method of caustics applied in viscoelastic fracture analysis[J]. *Optics and Lasers in Engineering*, 2011, **49**(5): 632-639. DOI:10.1016/j.optlaseng.2011.01.012.

基体裂纹-异型夹杂相互作用动态焦散线实验研究

岳中文[1] 韩瑞杰[1] 张 旺[1] 刘 伟[2]

([1]中国矿业大学(北京)力学与建筑工程学院, 北京 100083)
([2]清华大学工程力学系, 北京 100084)

摘要:将动态焦散线方法与高速摄影技术相结合,研究了低速冲击载荷作用下3种异型夹杂(方形夹杂、圆形夹杂和三角形夹杂)与基体裂纹的相互作用.通过记录不同夹杂情况下裂纹尖端自起裂到贯穿的动态焦散斑图,分析了Ⅰ型裂纹的动态应力强度因子 K_{I}^{d} 和裂纹扩展速率 v 与时间的关系. 实验结果表明:不同形状的夹杂会对裂纹尖端产生不同的阻裂效果,其中方形夹杂阻裂效果最明显;裂纹尖端焦散斑的畸变程度受到试件中夹杂形状的影响,圆形和方形夹杂对裂尖焦散斑畸变影响程度较大;三角形夹杂试件在裂纹扩展过程中裂尖动态应力强度因子值普遍高于圆形与方形夹杂试件,3组试件在断裂过程中裂尖由于受到反射波的扰动,其扩展速度、特征尺寸和动态应力强度因子值均呈现一定的波动性.研究结果为含异型夹杂构件的强度设计及抗冲击性能评估提供了依据.

关键词:动态焦散线;异形夹杂;动态应力强度因子;裂纹扩展速率
中图分类号:O346.1